NANJING UNIVERSITY

Impact of Quark Compositions in Sigma Mesons on Nuclear Matter and Neutron Star

Presenter: Yao Ma (马垚)

In collaboration with Prof. Yong-Liang Ma (马永亮)

Lanzhou University, Lanzhou, Mar. 22nd

Outline

- Motivation (Phenomenons and theories for dense nuclear matter)

- Theoretical framework and phenomenological analysis (Nuclear matter properties and neutron star structures with an extended linear sigma model (mixing picture between 2- and 4-quark configurations of scalar mesons))

- Summary and outlook

誠樸雄偉 勵學敦行

Motivation

Rich phenomenons of dense environments

Weak parameterizations in past studies on nuclear matter

Nuclei structures (low/intermediate densities)

- Hadron interactions around saturation density $n_0 = 0.16\mathrm{fm}^{-3}$ are crucial to nuclei structures, e.g. $^{24}\mathrm{Mg}$, $^{90}\mathrm{Zr}$, $^{116}\mathrm{Sn}$ and ^{208} Pb

B. A. Li and C. M. Ko, Nucl. Phys. A 618, 498 (1997).
D. H. Youngblood, H. L. Clark, and Y. W. Lui, Phys. Rev. Lett. 82, 691 (1999).
A. W. Steiner and B. A. Li, Phys. Rev. C 72, 041601 (2005).
L. W. Chen, C. M. Ko, and B. A. Li, Phys. Rev. C 72, 064309 (2005).
A. E. L. Dieperink, Y. Dewulf, D. Van Neck, M. Waroquier, and V. Rodin, Phys. Rev. C 68, 064307 (2003).
S. Karataglidis, K. Amos, B. A. Brown, and P. K. Deb, Phys. Rev. C 65, 044306 (2002).
R. J. Furnstahl, Nucl. Phys. A 706, 85 (2002).
B. A. Brown, Phys. Rev. Lett. 85, 5296 (2000).

$$E(n,\alpha) = E_0(n) + E_{\mathrm{sym}}(n)\alpha^2 + O\left(\alpha^4\right)$$

$$\alpha = \left(n_n - n_p\right)/\left(n_n + n_p\right)$$

$$n = n_n + n_p$$

$$E_0(n) = E_0\left(n_0\right) + \frac{K_0}{2!}\chi^2 + \frac{J_0}{3!}\chi^3 + O\left(\chi^4\right)$$

A. Sedrakian, J. J. Li, and F. Weber, Prog. Part. Nucl. Phys. 131, 104041 (2023)
M. Dutra, *et.al,* Phys. Rev. C 85, 035201 (2012).
J. M. Lattimer and Y. Lim, Astrophys. J. 771, 51 (2013).
M. Farine, J. M. Pearson, and F. Tondeur, Nucl. Phys. A 615, 135 (1997).

$$E_{\mathrm{sym}}(n) = E_{\mathrm{sym}}\left(n_r\right) + L\left(n_r\right)\chi_r + O\left(\chi_r^2\right)$$

$$\chi \equiv \left(n - n_0\right)/3n_0$$

$$\mathscr{L}_I = \bar{\psi}\left[i\gamma_\mu\partial^\mu - M - g_\sigma\sigma - g_\omega\gamma_\mu\omega^\mu - g_\rho\gamma_\mu\tau_a\rho^{a\mu}\right]\psi$$

$$n_0 \to 0.155 \pm 0.050\left(\mathrm{fm}^{-3}\right)$$
$$E_0(n_0) \to -15.0 \pm 1.0(\mathrm{MeV})$$
$$E_{\mathrm{sym}}(n_0) \to 30.9 \pm 1.9(\mathrm{MeV})$$
$$K_0 \to 230 \pm 30(\mathrm{MeV})$$
$$L_0 \to 52.5 \pm 17.5(\mathrm{MeV})$$
$$J_0 \to -700 \pm 500(\mathrm{MeV})$$

Neutron star (high densities)

嚴謹求實
勤奮創新

- The density in the cores of NSs always reach nearly $8n_0$
- M-R relations/ tidal deformations are sensitive to the EOS behavior throughout the whole density regions

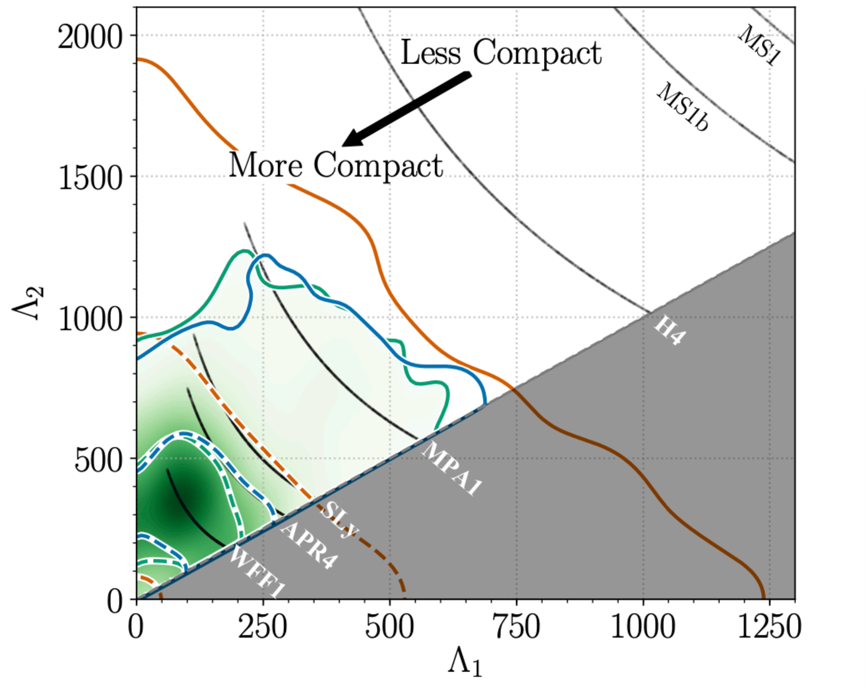

FIG. 1. Marginalized posterior for the tidal deformabilities of the two binary components of GW170817. The green shading shows the posterior obtained using the $\Lambda_a(\Lambda_s, q)$ EOS-insensitive relation to impose a common EOS for the two bodies, while the green, blue, and orange lines denote 50% (dashed) and 90% (solid) credible levels for the posteriors obtained using EOS-insensitive relations, a parametrized EOS without a maximum mass requirement, and independent EOSs (taken from [52]), respectively. The gray shading corresponds to the unphysical region $\Lambda_2 < \Lambda_1$ while the seven black scatter regions give the tidal parameters predicted by characteristic EOS models for this event [113, 115, 121–125].

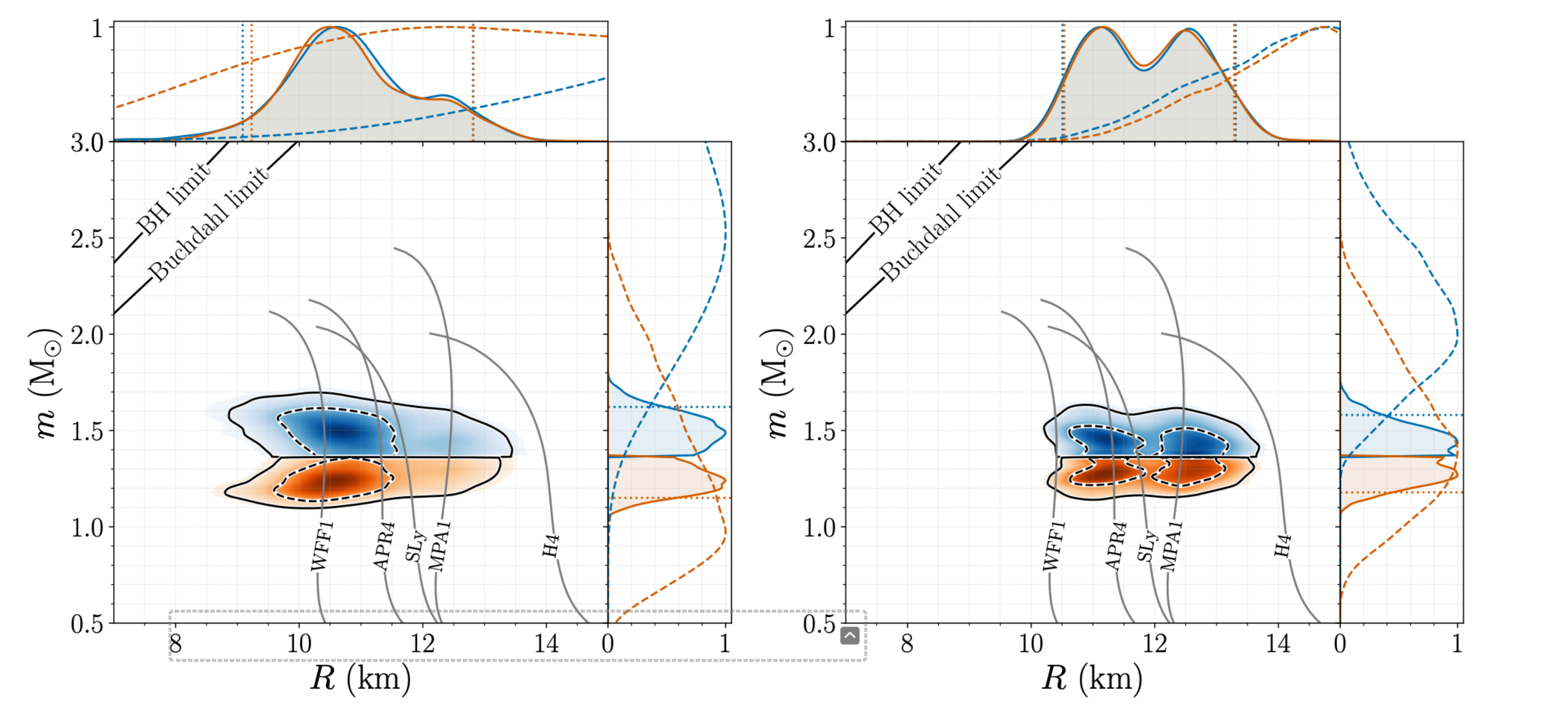

FIG. 3. Marginalized posterior for the mass m and areal radius R of each binary component using EOS-insensitive relations (left panel) and a parametrized EOS where we impose a lower limit on the maximum mass of 1.97 $M_\odot$ (right panel). The top blue (bottom orange) posterior corresponds to the heavier (lighter) NS. Example mass-radius curves for selected EOSs are overplotted in gray. The lines in the top left denote the Schwarzschild BH ($R = 2m$) and Buchdahl ($R = 9m/4$) limits. In the one-dimensional plots, solid lines are used for the posteriors, while dashed lines are used for the corresponding parameter priors. Dotted vertical lines are used for the bounds of the 90% credible intervals.

TOV equation

TABLE I. Source properties for GW170817: we give ranges encompassing the 90% credible intervals for different assumptions of the waveform model to bound systematic uncertainty. The mass values are quoted in the frame of the source, accounting for uncertainty in the source redshift.

	Low-spin priors ($\lvert\chi\rvert \le 0.05$)	High-spin priors ($\lvert\chi\rvert \le 0.89$)
Primary mass m_1	1.36–1.60 $M_\odot$	1.36–2.26 $M_\odot$
Secondary mass m_2	1.17–1.36 $M_\odot$	0.86–1.36 $M_\odot$
Chirp mass $\mathcal{M}$	$1.188^{+0.004}_{-0.002} M_\odot$	$1.188^{+0.004}_{-0.002} M_\odot$
Mass ratio m_2/m_1	0.7–1.0	0.4–1.0
Total mass $m_{\rm tot}$	$2.74^{+0.04}_{-0.01} M_\odot$	$2.82^{+0.47}_{-0.09} M_\odot$
Radiated energy $E_{\rm rad}$	$> 0.025 M_\odot c^2$	$> 0.025 M_\odot c^2$
Luminosity distance $D_{\rm L}$	40^{+8}_{-14} Mpc	40^{+8}_{-14} Mpc
Viewing angle Θ	$\le 55°$	$\le 56°$
Using NGC 4993 location	$\le 28°$	$\le 28°$
Combined dimensionless tidal deformability $\tilde\Lambda$	≤ 800	≤ 700
Dimensionless tidal deformability $\Lambda(1.4M_\odot)$	≤ 800	≤ 1400

B. P. Abbott et al. (LIGO Scientific, Virgo), Phys. Rev. Lett. 119, 161101 (2017)
B. P. Abbott et al. (LIGO Scientific, Virgo), Phys. Rev. Lett. 121, 161101 (2018)

Polytropic process +estimations of strong interaction + TOV equation

R. C. Tolman, Phys. Rev. 55, 364 (1939).
J. R. Oppenheimer and G. M. Volkoff, Phys. Rev. 55, 374 (1939).

δ meson effects

嚴謹求實
勤奮創新

T. Miyatsu, M.-K. Cheoun, and K. Saito, Astrophys. J. 929, 82 (2022).

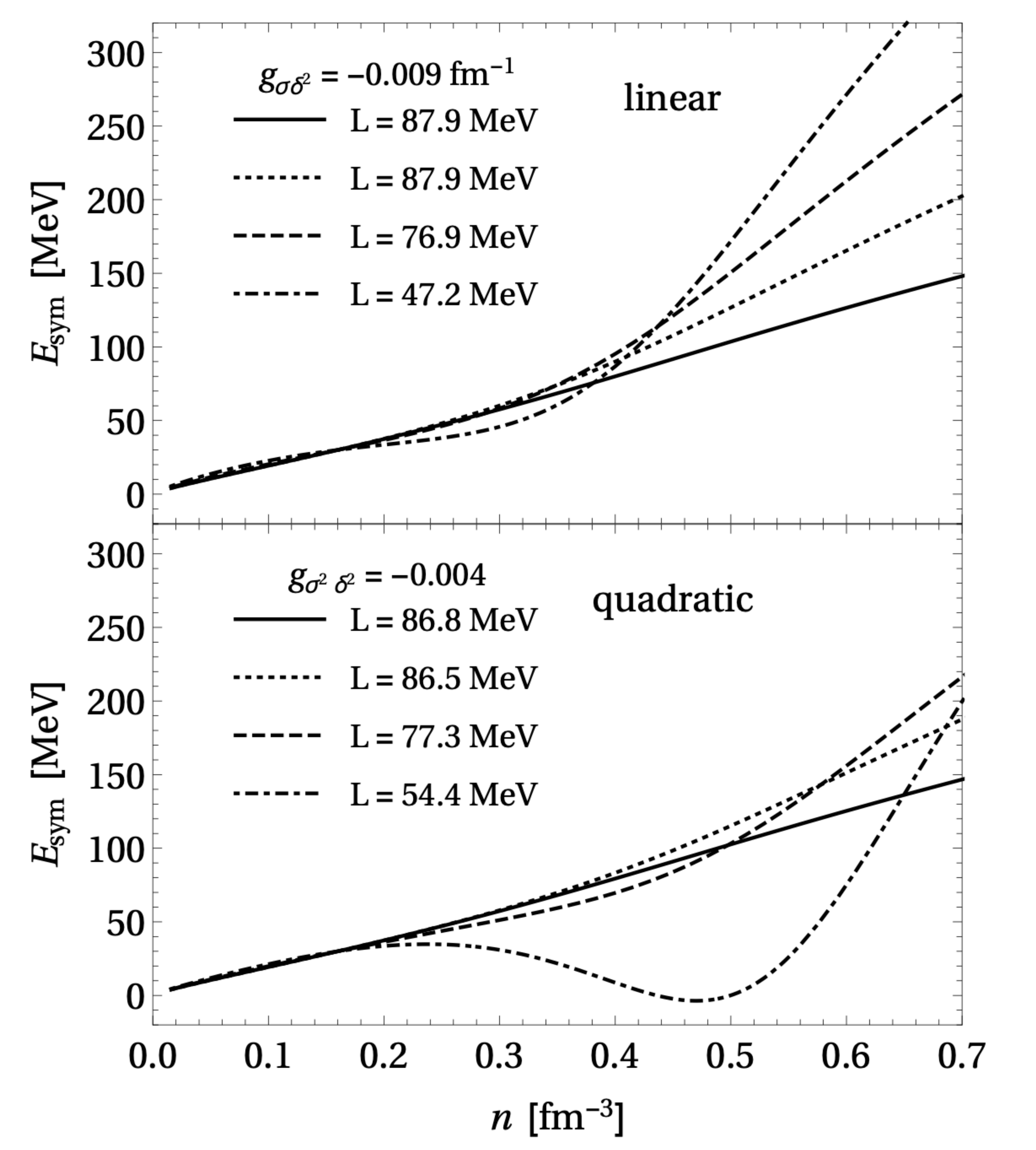

FIG. 2. Symmetry energy E_{sym} for negative value of g_α with respect to various values of C_δ^2 for both types of coupling.

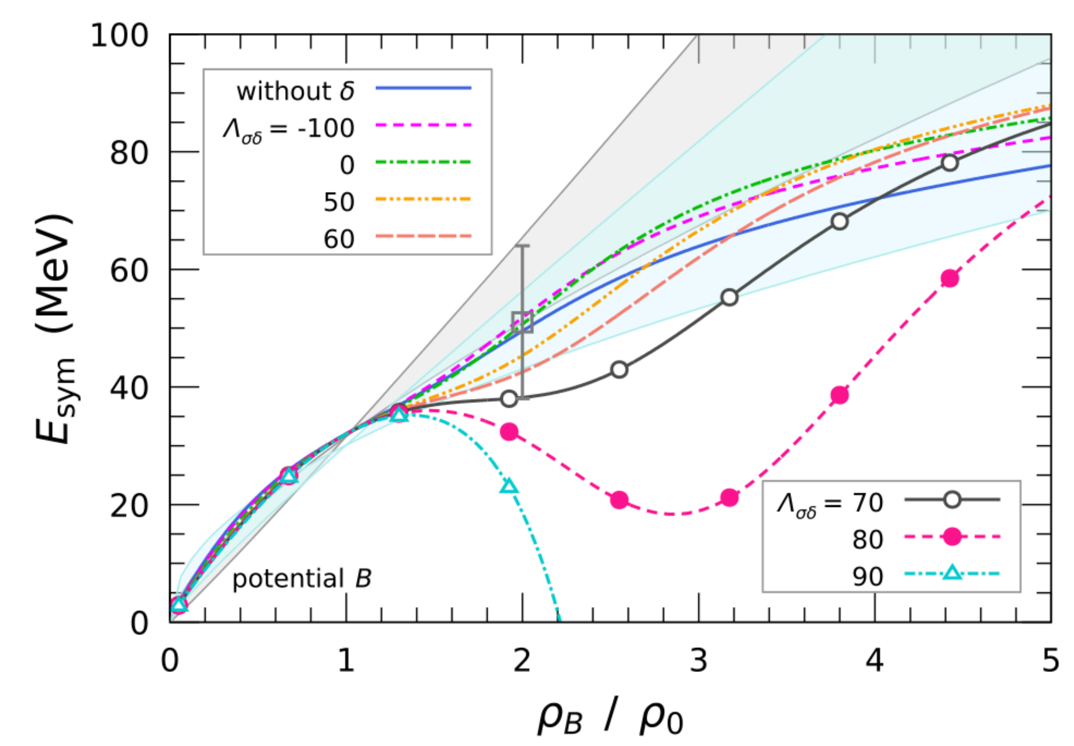

Figure 4. Same as Figure 3 but with the σ-δ mixing. The coupling constants in potential B are used.

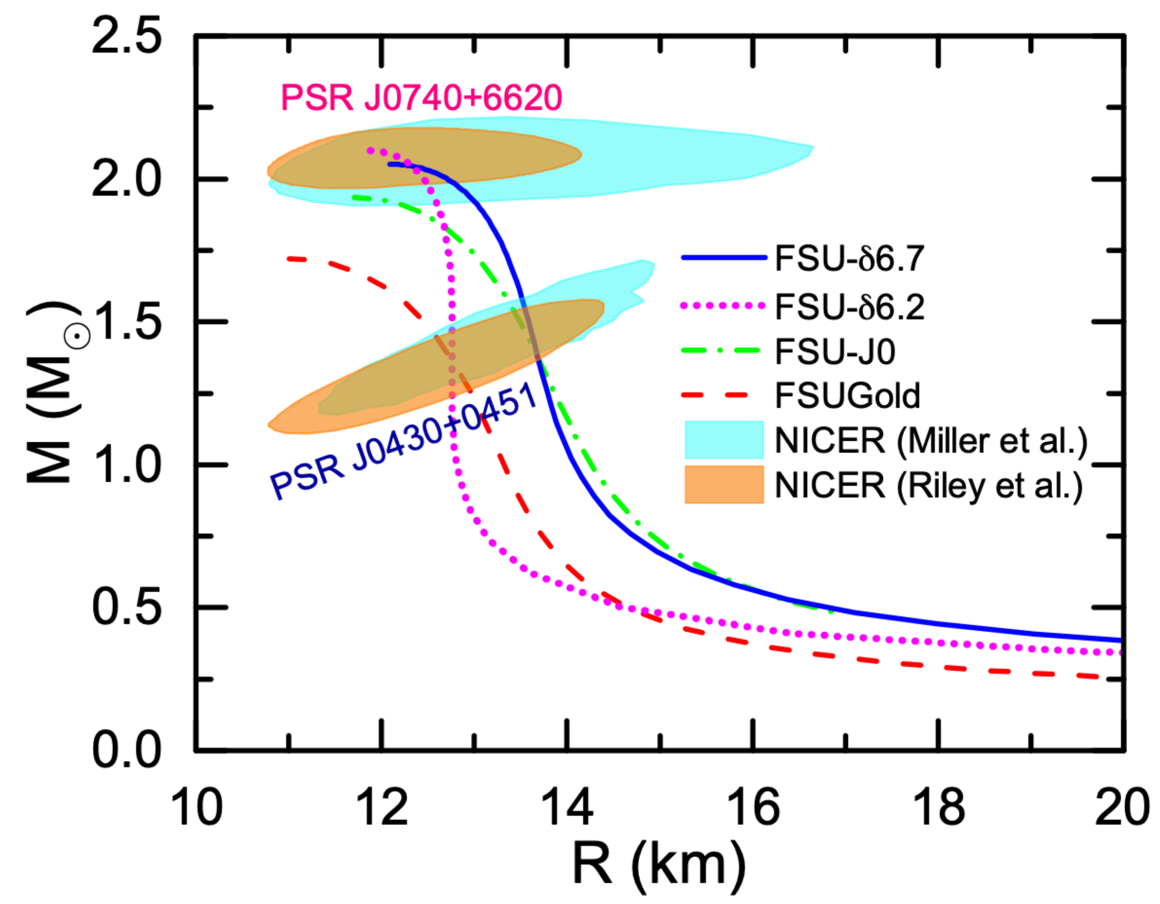

Figure 2. M-R relation for static NSs from FSUGold, FSU-J0, FSU-δ6.7 and FSU-δ6.2. The NICER (XMM-Newton) constraints with 68% C.L for PSR J0030+0451 (Riley et al. 2019; Miller et al. 2019) and PSR J0740+6620 (Riley et al. 2021; Miller et al. 2021) are also included for comparison.

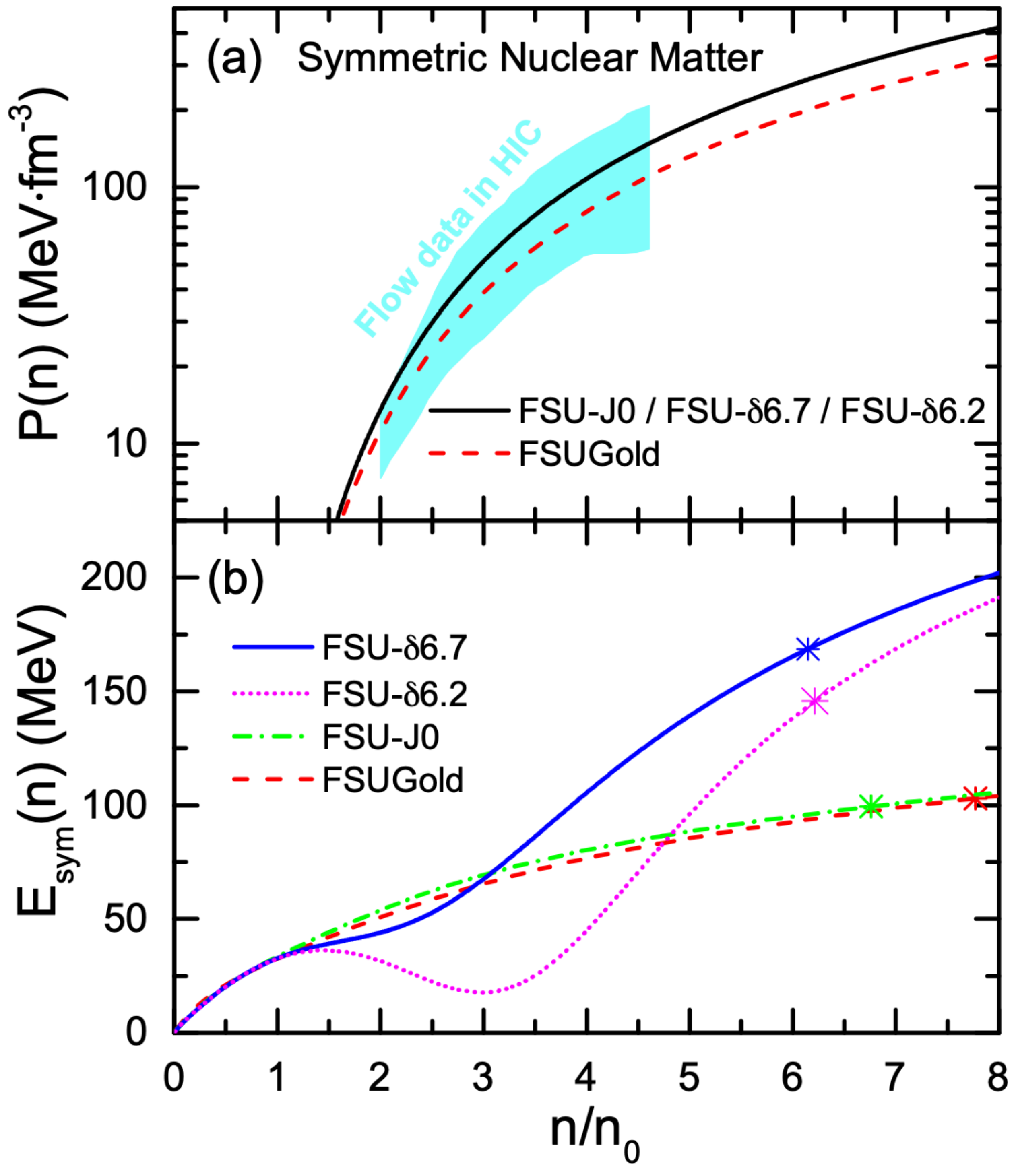

Figure 1. Pressure vs density (a) and density dependence of the symmetry energy (b) predicted by FSUGold, FSU-J0, FSU-δ6.7 and FSU-δ6.2. The shaded area in panel (a) represents the constraints from flow data in heavy-ion collisions (Danielewicz et al. 2002). The central density of maximum mass NS configuration is indicated by '∗' in panel (b).

N. Zabari, S. Kubis, and W. Wójcik, Phys. Rev. C 99, 035209 (2019).

F. Li, B.-J. Cai, Y. Zhou, W.-Z. Jiang, and L.-W. Chen, Astrophys. J. 929, 183 (2022).

Hyperon effects (Strangeness)

嚴謹求實 勤奮創新

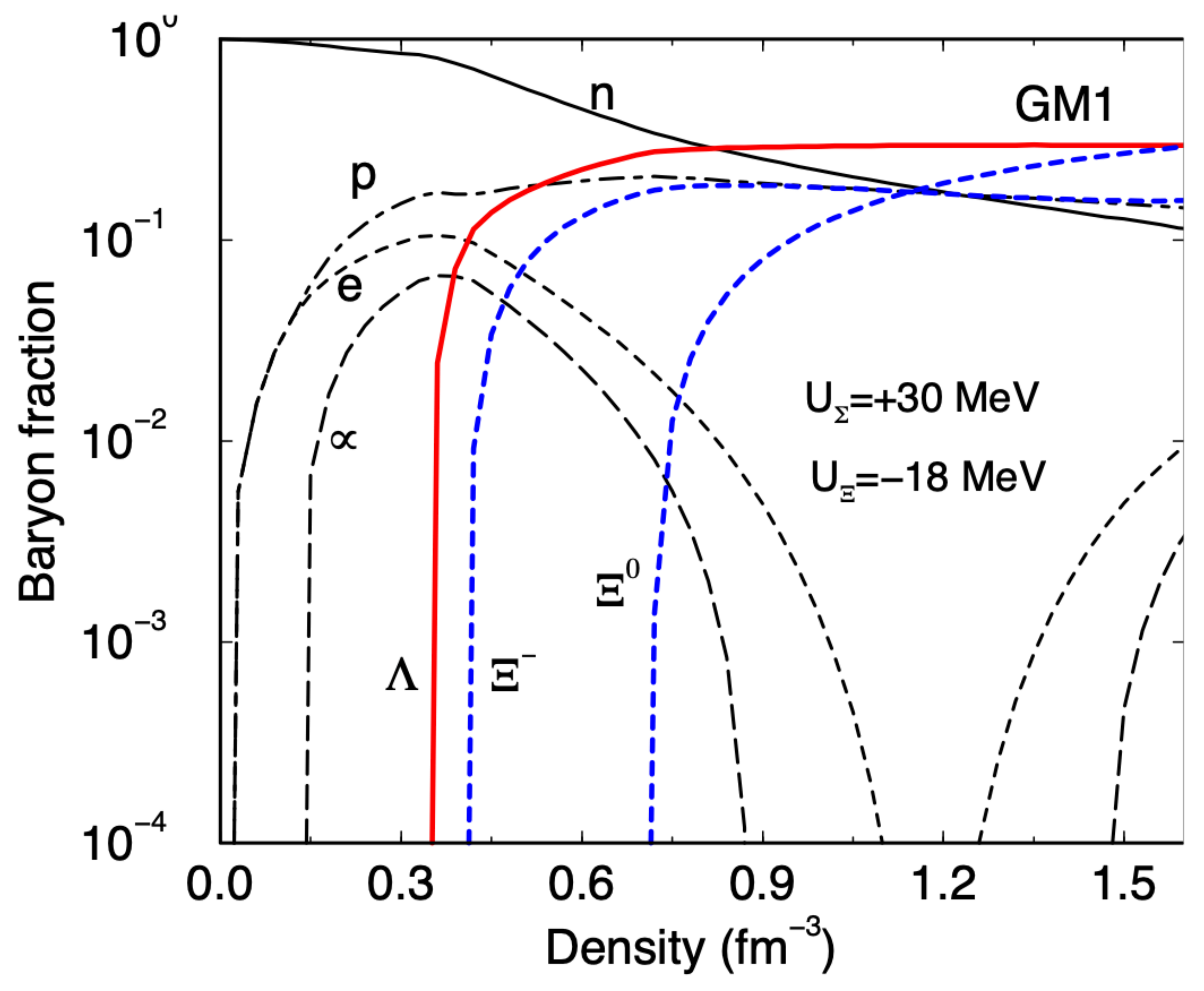

FIG. 31 Neutron star matter fractions of baryons and leptons, calculated as a function of density. From Schaffner-Bielich, 2008.

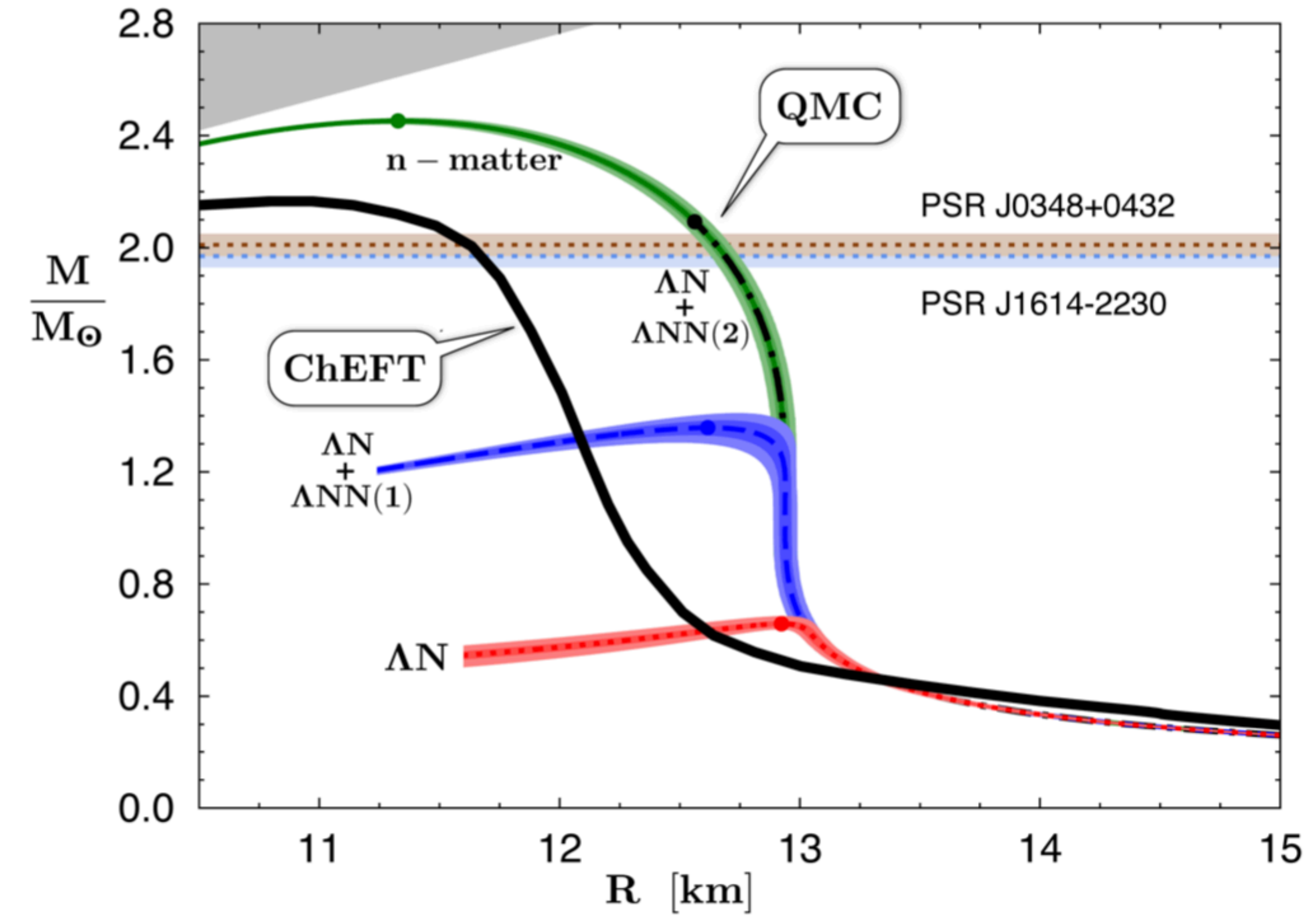

FIG. 33 Mass-radius relationship for various EoS scenarios of neutron stars, including nucleons and leptons only (Hell and Weise, 2014) as well as upon including Λ hyperons (Lonardoni *et al.*, 2015). From Weise, 2015.

A. Gal, E. V. Hungerford, and D. J. Millener, Rev. Mod. Phys. 88, 035004 (2016).

Chemical potential equilibrium, e.g. $\mu_\Lambda = \mu_p + \mu_e$

Method to handle dense system

1. Relativistic mean field approximation

J. D. Walecka, Ann. Phys. **83**, 491 (1974).

$$\mathscr{L} = \mathscr{L}_{\mathrm{N}} + \mathscr{L}_{\sigma} + \mathscr{L}_{\omega} + \mathscr{L}_{\mathrm{I}}$$

$$\mathscr{L}_{\mathrm{N}} = \bar{\psi}\left(\mathrm{i}\gamma_\mu\partial^\mu - m_{\mathrm{N}}\right)\psi$$

$$\mathscr{L}_{\sigma} = \frac{1}{2}\left(\partial_\mu\phi\partial^\mu\phi - m_\sigma^2\phi^2\right)$$

$$\mathscr{L}_{\omega} = -\frac{1}{4}W_{\mu\nu}W^{\mu\nu} + \frac{1}{2}m_\omega^2\omega_\mu\omega^\mu$$

$$\mathscr{L}_{\mathrm{I}} = \mathscr{L}_{\sigma\mathrm{N}} + \mathscr{L}_{\omega\mathrm{N}} = g_\sigma\phi\bar{\psi}\psi - g_\omega\omega^\mu\bar{\psi}\gamma_\mu\psi$$

$$\left(\mathrm{i}\gamma_\mu\partial^\mu - g_\omega\gamma_0\omega^0 - m_{\mathrm{N}}\right)\psi = 0, \quad m_{\mathrm{N}}^* = m_{\mathrm{N}} - g_\sigma\phi,$$

$$\phi = \frac{g_\sigma}{m_\sigma^2}\rho_{\mathrm{s}}, \quad \rho_{\mathrm{s}} = \langle\bar{\psi}\psi\rangle,$$

$$\omega^0 = \frac{g_\omega}{m_\omega^2}\rho_{\mathrm{B}}, \quad \rho_{\mathrm{B}} = \left\langle\psi^\dagger\psi\right\rangle,$$

2. Relativistic Hartree-Fock method

$$\mathscr{L}_I = -g_\sigma\bar{\psi}\sigma\psi - g_\omega\bar{\psi}\gamma_\mu\omega^\mu\psi + \frac{f_\omega}{2M}\bar{\psi}\sigma_{\mu\nu}\partial^\nu\omega^\mu\psi$$
$$-g_\rho\bar{\psi}\gamma_\mu\rho^\mu\cdot\tau\psi + \frac{f_\rho}{2M}\bar{\psi}\sigma_{\mu\nu}\partial^\nu\rho^\mu\cdot\tau\psi$$
$$-e\bar{\psi}\gamma_\mu\frac{1}{2}\left(1+\tau_3\right)A^\mu\psi + \mathscr{L}_{\pi\mathrm{NN}}$$

$$\Sigma(\mathbf{p}) = \Sigma_S(p) + \gamma_0\Sigma_0(p) + \gamma\cdot\hat{\mathbf{p}}\Sigma_V(p)$$

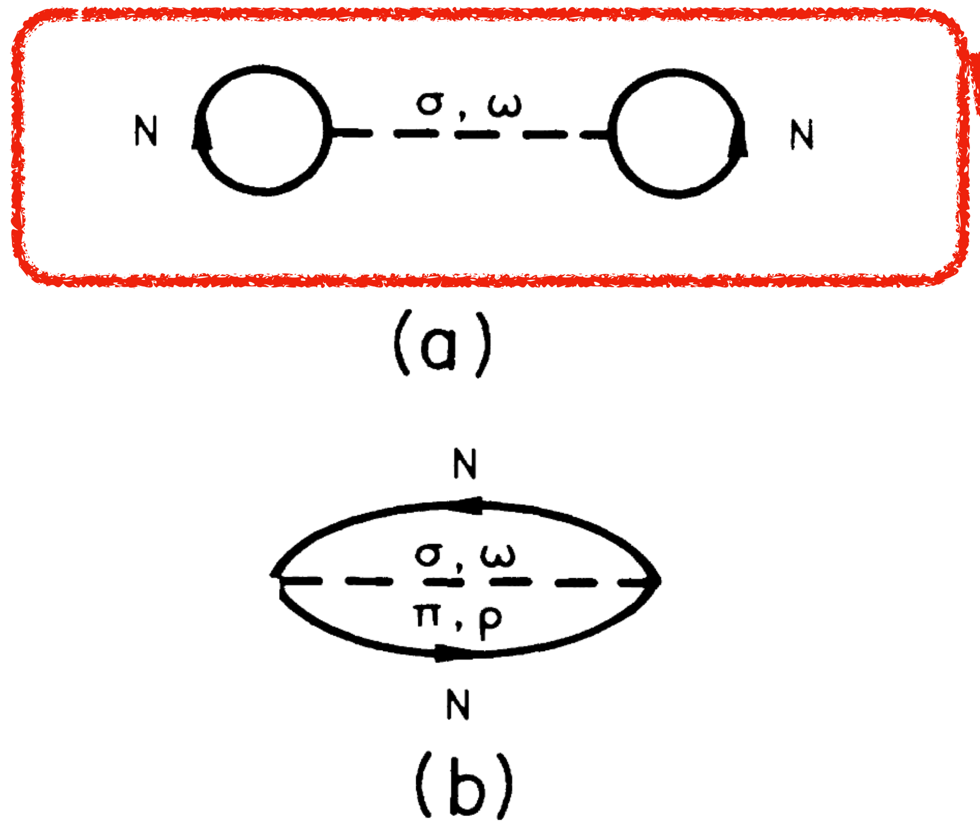

A. Bouyssy, J.-F. Mathiot, N. V. Giai, and S. Marcos, Phys Rev C **36**, 380 (1987).

誠樸雄偉 勵學敦行

Can we extend an EFT/model taking care of QCD symmetry patterns into dense nucleon systems?

An extended linear sigma model in nuclear matter

Phys. Rev. D 109 (2024) 7, 7, **YM** and Y. L. Ma

P-wave problems in light scalar meson sectors below 1GeV

F. E. Close and N. A. Tornqvist, J. Phys. G 28, R249 (2002)

↓

A tetra-quark picture to include δ ($a_0(980)$) meson and hyperon

Freedoms to be considered

- Highlights of the parametrization:

I. Include meson exchanges, e.g. $f_0(500)(\sigma)$ and $a_0(980)(\delta)$

II. Include baryon freedoms, e.g. nucleon and hyperon

$$R^\mu = V^\mu - A^\mu = \frac{1}{\sqrt{2}}\begin{pmatrix} \frac{\omega_N^\mu+\rho^{\mu 0}}{\sqrt{2}} - \frac{f_{1N}^\mu+a_1^{\mu 0}}{\sqrt{2}} & \rho^{\mu+} - a_1^{\mu+} & K^{*\mu+} - K_1^{\mu+} \\ \rho^{\mu-} - a_1^{\mu-} & \frac{\omega_N^\mu-\rho^{\mu 0}}{\sqrt{2}} - \frac{f_{1N}^\mu-a_1^{\mu 0}}{\sqrt{2}} & K^{*\mu 0} - K_1^{\mu 0} \\ K^{*\mu-} - K_1^{\mu-} & \bar{K}^{*\mu 0} - \bar{K}_1^{\mu 0} & \omega_S^\mu - f_{1S}^\mu \end{pmatrix}$$

$$L^\mu = V^\mu + A^\mu = \frac{1}{\sqrt{2}}\begin{pmatrix} \frac{\omega_N^\mu+\rho^{\mu 0}}{\sqrt{2}} + \frac{f_{1N}^\mu+a_1^{\mu 0}}{\sqrt{2}} & \rho^{\mu+} + a_1^{\mu+} & K^{*\mu+} + K_1^{\mu+} \\ \rho^{\mu-} + a_1^{\mu-} & \frac{\omega_N^\mu-\rho^{\mu 0}}{\sqrt{2}} + \frac{f_{1N}^\mu-a_1^{\mu 0}}{\sqrt{2}} & K^{*\mu 0} + K_1^{\mu 0} \\ K^{*\mu-} + K_1^{\mu-} & \bar{K}^{*\mu 0} + \bar{K}_1^{\mu 0} & \omega_S^\mu + f_{1S}^\mu \end{pmatrix}$$

$$\Phi = S + iP = \begin{pmatrix} \frac{(\sigma_N+a_0^0)+i(\eta_N+\pi^0)}{\sqrt{2}} & a_0^+ + i\pi^+ & K_S^+ + iK^+ \\ a_0^- + i\pi^- & \frac{(\sigma_N-a_0^0)+i(\eta_N-\pi^0)}{\sqrt{2}} & K_S^0 + iK^0 \\ K_S^- + iK^- & \bar{K}_S^0 + i\bar{K}^0 & \sigma_S + i\eta_S \end{pmatrix}$$

a_0 mesons may be crucial to NS tidal deformations and neutron skin of nucleus

D. Adhikari et al. (PREX), Phys. Rev. Lett. 126, 172502 (2021)
B. T. Reed, F. J. Fattoyev, C. J. Horowitz, and J. Piekarewicz, Phys. Rev. Lett. 126, 172503 (2021)
F. Li, B. J. Cai, Y. Zhou, W. Z. Jiang, and L. W. Chen, Astrophys. J. 929, 183 (2022)

$$B_N \equiv \begin{pmatrix} \frac{\Lambda}{\sqrt{6}} + \frac{\Sigma^0}{\sqrt{2}} & \Sigma^+ & p \\ \Sigma^- & \frac{\Lambda}{\sqrt{6}} - \frac{\Sigma^0}{\sqrt{2}} & n \\ \Xi^- & \Xi^0 & -\frac{2\Lambda}{\sqrt{6}} \end{pmatrix}$$

High densities may lead to hyperon cores of NSs

N. K. Glendenning, Astrophys. J. 293, 470 (1985)
N. K. Glendenning and S. A. Moszkowski, Phys. Rev. Lett. 67, 2414 (1991).
S. Weissenborn, D. Chatterjee, and J. Schaffner-Bielich, Phys. Rev. C 85, 065802 (2012), [Erratum: Phys. Rev. C 90, 019904 (2014)]

The chiral transformations

$SU(3)_R \otimes SU(3)_L$

$$\Phi' \to g_L \Phi' g_R^\dagger, \quad \hat{\Phi}' \to g_L \hat{\Phi}' g_R^\dagger$$

$$L_\mu \to g_L L_\mu g_L^\dagger, \quad R_\mu \to g_R R_\mu g_R^\dagger$$

$$N_R^{(RR)} \to g_R N_R^{(RR)} g_R^\dagger$$

$$N_R^{(LL)} \to g_R N_R^{(LL)} g_L^\dagger$$

$U(1)_A$

2-quark

4-quark

$$\Phi' \to e^{2i\nu} \Phi', \quad \hat{\Phi}' \to e^{-4i\nu} \hat{\Phi}',$$

$$L_\mu \to L_\mu, \quad R_\mu \to R_\mu$$

$$N_R^{(RR)} \to e^{-3i\nu} N_R^{(RR)}, \quad N_L^{(RR)} \to e^{-i\nu} N_L^{(RR)}$$

$$N_R^{(LL)} \to e^{i\nu} N_R^{(LL)}, \quad N_L^{(LL)} \to e^{3i\nu} N_L^{(LL)}$$

di-quark approximation

Power counting rules

① The operators are limited within dimension-4, for the higher dimensional operators are suppressed by the cutoff scale;

② The quark number of an operator is limited within 8 and the number of flavor space traces is limited to only 1, for its suppression by N_c;

③ The explicit symmetry breaking caused by quark mass is treated as perturbation, and it's ignored in current work.

A. H. Fariborz, R. Jora, and J. Schechter, Phys. Rev. D 77, 034006 (2008).
A. H. Fariborz, R. Jora, and J. Schechter, Phys. Rev. D 72, 034001 (2005)
A. H. Fariborz, R. Jora, and J. Schechter, Phys. Rev. D 79, 074014 (2009)
D. Parganlija, F. Giacosa, and D. H. Rischke, Phys. Rev. D 82, 054024 (2010)

The lowest order Lagrangians

$$\mathscr{L}_{\mathrm{M}} = \frac{1}{2}\mathrm{Tr}\left(\partial_\mu \Phi' \partial^\mu \Phi'^\dagger\right) + \frac{1}{2}\mathrm{Tr}\left(\partial_\mu \hat{\Phi}' \partial^\mu \hat{\Phi}'^\dagger\right) + c_2\,\mathrm{Tr}\left(\Phi'\Phi'^\dagger\right) - c_4\,\mathrm{Tr}\left(\Phi'\Phi'^\dagger\Phi'\Phi'^\dagger\right) - d_2\,\mathrm{Tr}\left(\hat{\Phi}'\hat{\Phi}'^\dagger\right) -$$

$$e_3\left(\epsilon_{abc}\epsilon^{def}\Phi'^a_d\Phi'^b_e\hat{\Phi}'^c_f + \text{ h.c. }\right) - c_3\left[\gamma_1 \ln\left(\frac{\det\Phi'}{\det\hat{\Phi}'^\dagger}\right) + \left(1-\gamma_1\right)\ln\left(\frac{\mathrm{Tr}\left(\Phi'\hat{\Phi}'^\dagger\right)}{\mathrm{Tr}\left(\hat{\Phi}'\Phi'^\dagger\right)}\right)\right]^2$$

A. H. Fariborz, R. Jora, and J. Schechter, Phys. Rev. D 72, 034001 (2005)
A. H. Fariborz, R. Jora, and J. Schechter, Phys. Rev. D 77, 034006 (2008)
A. H. Fariborz, R. Jora, and J. Schechter, Phys. Rev. D 79, 074014 (2009)

$$
\begin{aligned}
\mathscr{L}_{\mathrm{V}} = &-\frac{1}{8}\mathrm{Tr}\left(L_{\mu\nu}L^{\mu\nu}+R_{\mu\nu}R^{\mu\nu}\right)+g_1\left[\mathrm{Tr}\left(\partial_\nu R_\mu R^\mu R^\nu\right)+\mathrm{Tr}\left(\partial_\nu L_\mu L^\mu L^\nu\right)\right]+\\
&g_2\left[\mathrm{Tr}\left(\partial_\nu R_\mu R^\nu R^\mu\right)+\mathrm{Tr}\left(\partial_\nu L_\mu L^\nu L^\mu\right)\right]+g_3\left[\mathrm{Tr}\left(R_\mu R^\mu R_\nu R^\nu\right)+\mathrm{Tr}\left(L_\mu L^\mu L_\nu L^\nu\right)\right]+\\
&g_4\left[\mathrm{Tr}\left(R_\mu R^\nu R_\mu R^\nu\right)+\mathrm{Tr}\left(L_\mu L^\nu L_\mu L^\nu\right)\right]+h_1\left[\mathrm{Tr}\left(\Phi'^\dagger\Phi' R_\mu R^\mu\right)+\mathrm{Tr}\left(\Phi'\Phi'^\dagger L_\mu L^\mu\right)\right]+\\
&h_2\left[\mathrm{Tr}\left(L^\mu\Phi' R_\mu\Phi'^\dagger\right)\right]+h_3\left[\mathrm{Tr}\left(\Phi'^\dagger\partial_\mu\Phi' R^\mu\right)+\mathrm{Tr}\left(\Phi'\partial_\mu\Phi'^\dagger L^\mu\right)\right]+\\
&\frac{a_1}{2}\epsilon_{abc}\epsilon^{def}\left[\left(R_\mu\right)_{ad}\left(R_\nu\right)_{be}\left(\Phi'^\dagger\Phi\right)_{cf}+\left(L_\mu\right)_{ad}\left(L_\nu\right)_{be}\left(\Phi\Phi'^\dagger\right)_{cf}\right]+\\
&\frac{a_2}{2}\epsilon_{abc}\epsilon^{\mathrm{def}}\left[\left(R_\mu\right)_{ad}\left(R_\nu\right)_{be}\left(R^\mu R^\nu\right)_{cf}+\left(L_\mu\right)_{ad}\left(L_\nu\right)_{be}\left(L^\mu L^\nu\right)_{cf}\right]+\\
&\frac{a_3}{2}\epsilon_{abc}\epsilon^{def}\left[\left(R_\mu\right)_{ad}\left(R^\mu\right)_{be}\left(R^\nu R_\nu\right)_{cf}+\left(L_\mu\right)_{ad}\left(L^\mu\right)_{be}\left(L^\nu L_\nu\right)_{cf}\right]+\\
&\frac{a_4}{2}\epsilon_{abc}\epsilon^{def}\left[\left(R_\mu\right)_{ad}\left(R^\nu\right)_{be}\left(\partial^\mu R_\nu\right)_{cf}+\left(L_\mu\right)_{ad}\left(L^\nu\right)_{be}\left(\partial^\mu L_\nu\right)_{cf}\right]
\end{aligned}
$$

Di-quark approximation

L. Olbrich, Master's thesis, Goethe U., Frankfurt (main) (2015).
L. Olbrich, M. Zétényi, F. Giacosa, and D. H. Rischke, Phys. Rev. D 93, 034021 (2016).

$$N_{\mathrm{R,\,L}}^{(\mathrm{RR})} = \frac{1}{\sqrt{2}} \frac{1 \pm \gamma_5}{2} B, \quad N_{\mathrm{R,\,L}}^{(\mathrm{LL})} = -\frac{1}{\sqrt{2}} \frac{1 \pm \gamma_5}{2} B$$

$$\mathscr{L}_{\mathrm{B}} = \mathrm{Tr}(\bar{B} i \not{\partial} B) + c\,\mathrm{Tr}\left(\bar{B}\gamma_\mu V^\mu B + \bar{B}\gamma_\mu\gamma_5 A^\mu B\right) + c'\,\mathrm{Tr}\left(\bar{B}\gamma_\mu \bar{B} V^\mu + \bar{B}\gamma_\mu\gamma_5 \bar{B} A^\mu\right) +$$

$$h\epsilon_{abc}\epsilon^{def}\left[(\bar{B})_{ad}\gamma_\mu(B)_{be}(V^\mu)_{cf} + (\bar{B})_{ad}\gamma_\mu\gamma_5(B)_{be}(A^\mu)_{cf}\right] -$$

$$\frac{g}{2}\mathrm{Tr}\left[\bar{B}\left(\Phi' + \Phi'^\dagger\right)B + \bar{B}\gamma_5\left(\Phi' - \Phi'^\dagger\right)B\right] -$$

$$\frac{e}{2}\epsilon_{abc}\epsilon^{def}\left[(\bar{B})_{ad}\left(\Phi' + \Phi'^\dagger\right)_{be}(B)_{cf} + (\bar{B})_{ad}\gamma_5\left(\Phi' - \Phi'^\dagger\right)_{be}(B)_{cf}\right]$$

The Lagrangian at the lowest order for RMF

$$\mathscr{V}_{\rm M} = c_2\,{\rm Tr}\,S'^2 - d_2\,{\rm Tr}\,\hat{S}'^2 - c_4\,{\rm Tr}\,S'^4 - 2e_3\epsilon_{abc}\epsilon_{def}S'_{ad}S'_{be}\hat{S}'_{cf}$$

$$\mathscr{V}_{\rm V} = \tilde{h}_2\,{\rm Tr}\left(S'^2V^2\right) + \tilde{g}_3\,{\rm Tr}\,V^4 + a_1\epsilon_{abc}\epsilon_{def}V_{ad}V_{be}\left(S'^2\right)_{cf}$$

$$\mathscr{L}_{\rm B}^{\rm RMF} = {\rm Tr}\left(\bar{B}i\gamma_\mu\partial^\mu B\right) + c\,{\rm Tr}\left(\bar{B}\gamma^0VB\right) - g\,{\rm Tr}\left(\bar{B}S'B\right) + h\epsilon_{abc}\epsilon_{def}\bar{B}_{ad}\gamma^0B_{be}V_{cf} - e\epsilon_{abc}\epsilon_{def}\bar{B}_{ad}\gamma^0B_{be}S'_{cf}$$

Phys. Rev. D 109 (2024) 7, 7, **YM** and Y. L. Ma

Improvement of parameter space

SSB of chiral symmetry

- Spontaneous symmetry breaking down from $\mathrm{SU(3)_L} \otimes \mathrm{SU(3)_R}$ to $\mathrm{SU(3)_V}$

$$\langle \sigma' \rangle = \sqrt{3}\alpha \text{ and } \langle \hat{\sigma}' \rangle = \sqrt{3}\beta$$

- Mixing between 2-quark and 4-quark configurations

$$\sigma = \cos\theta_0 \sigma' + \sin\theta_0 \hat{\sigma}'$$

$$a_0 = \cos\theta_8 a_0' + \sin\theta_8 \hat{a}_0{}'$$

$$f_0 = \cos\theta_8 f_0' + \sin\theta_8 \hat{f}_0{}'$$

Phenomenological analysis

Parameter space choice

	α(MeV)	β(MeV)	e_3(MeV)	c_4	h_2	$\tilde{g}_3$	c	g	a_1	$\tilde{g}$	e
el-g30eg	61.4	26.4	-2100	45.6	79.3	0.397	9.51	6.54	4.10	-2.61	8.75
el-g30e	61.1	24.4	-2050	43.6	80.0	0.542	11.4	0.234	4.17	-0.790	15.1
el-g30g	61.1	24.7	-2060	44.0	80.1	1.59	-0.792	15.4	4.25	11.5	-0.027
el-g350eg	61.2	25.6	-2100	44.4	79.9	51.5	10.1	6.35	4.14	-2.65	9
el-g3100eg	60.8	24.0	-2090	42.4	80.8	100	10.6	7.10	4.19	-2.88	8.34
el-g3150eg	60.7	24.3	-2110	42.0	81.0	150	11.1	7.15	4.18	-3.05	8.30

↔

	$g_{\sigma NN}$	g_{aNN}	g_{fNN}	$g_{\omega NN}$	$g_{\rho NN}$
el-g30eg	-5.98	-0.671	2.68	6.06	3.45
el-g30e	-6.20	-5.03	3.00	6.09	5.30
el-g30g	-6.17	5.12	2.95	-6.09	5.30
el-g350eg	-6.12	-0.852	2.85	6.37	3.71
el-g3100eg	-6.36	-0.442	3.19	6.73	3.85
el-g3150eg	-6.38	-0.413	3.20	7.09	4.04

Bare mass parameters and NM properties

嚴謹求實
勤奮創新

Y. Sugahara and H. Toki, Nucl. Phys. A579,557 (1994).
F. Li, B. J. Cai, Y. Zhou, W. Z. Jiang, and L. W. Chen, Astrophys. J. 929, 183 (2022).

Physical quantities in unit of MeV

	B.E.	E_{sym}	K_0	L_0	J_0	m_ρ	m_ω	m_σ	$m_{\sigma'}$	m_{a_0}	$m_{a_0'}$	m_N
Empirical	-15.0±1.0	30.9±1.9	250±50	52.5±17.5	-700±500	763±2	783±1	475±75	1350±100	995±25	1410±120	939±1
el-g30eg	-14.6	30.1	415	92.2	421	763	783	503	1520	977	1510	939
el-g30e	-14.6	31.6	420	85.8	479	763	783	525	1510	991	1480	939
el-g30g	-14.6	30.9	418	83.6	451	763	783	522	1510	989	1480	939
el-g350eg	-15.2	30.9	370	80.7	-392	763	783	498	1520	983	1500	939
el-g3100eg	-15.4	31.4	317	71.7	-1020	763	783	502	1510	994	1470	939
el-g3150eg	-15.6	31.6	253	63.7	-1470	763	783	485	1510	991	1470	939
TM1	-16.3	36.9	280	113	-247	770	783	511	—	—	—	938
$\text{FSU}-\delta 6.7$	-16.3	32.7	229	53.5	-322	763	783	492	—	980	—	938

A. Sedrakian, J. J. Li, and F. Weber, Prog. Part. Nucl. Phys. 131, 104041 (2023).
J. M. Lattimer and Y. Lim, Astrophys. J. 771, 51 (2013).
M. Farine, J. M. Pearson, and F. Tondeur, Nucl. Phys. A 615, 135 (1997).
M. Dutra, et al., Phys. Rev. C 85, 035201 (2012).

R. L. Workman, et al. (Particle Data Group), PTEP 2022, 083C01 (2022).

Comparison among different g_3 cases

嚴謹求實
勤奮創新

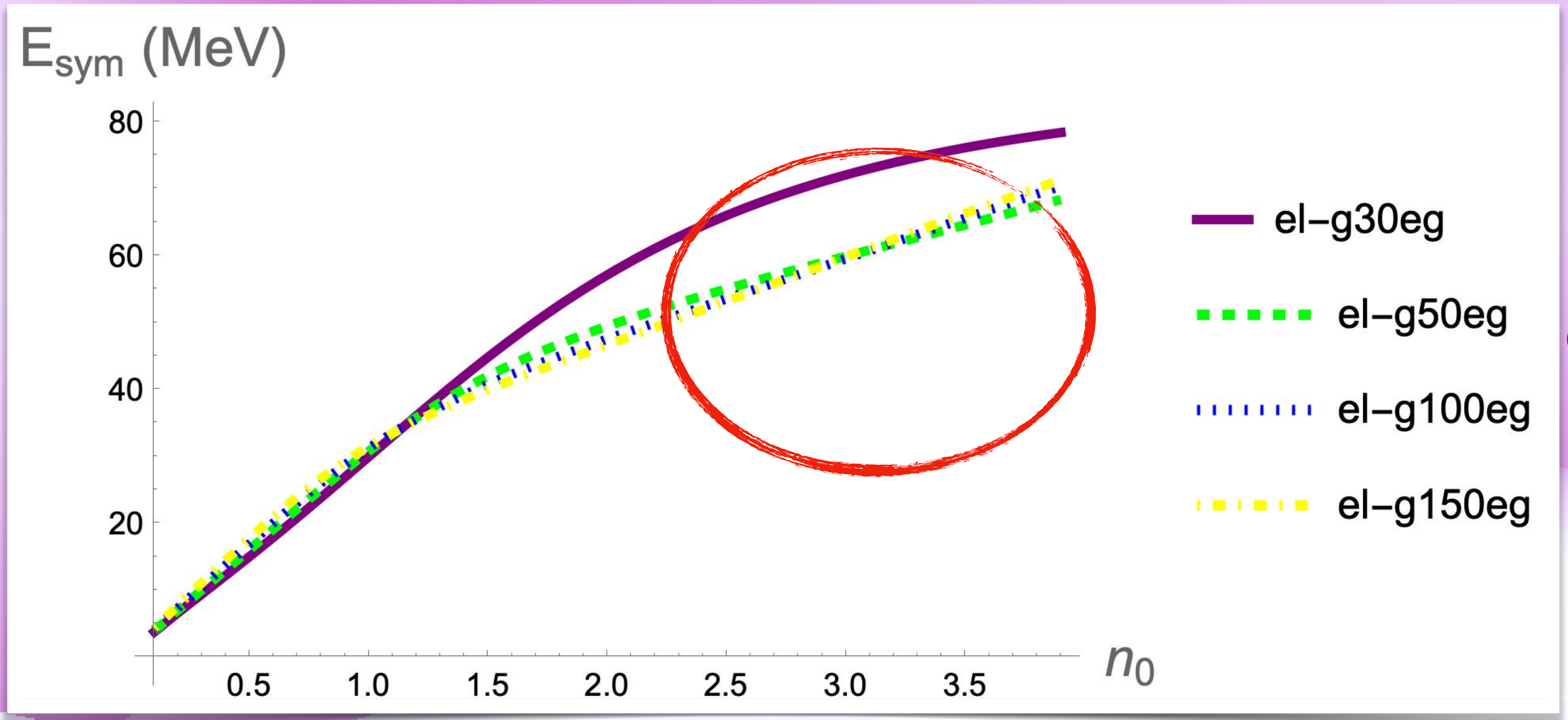

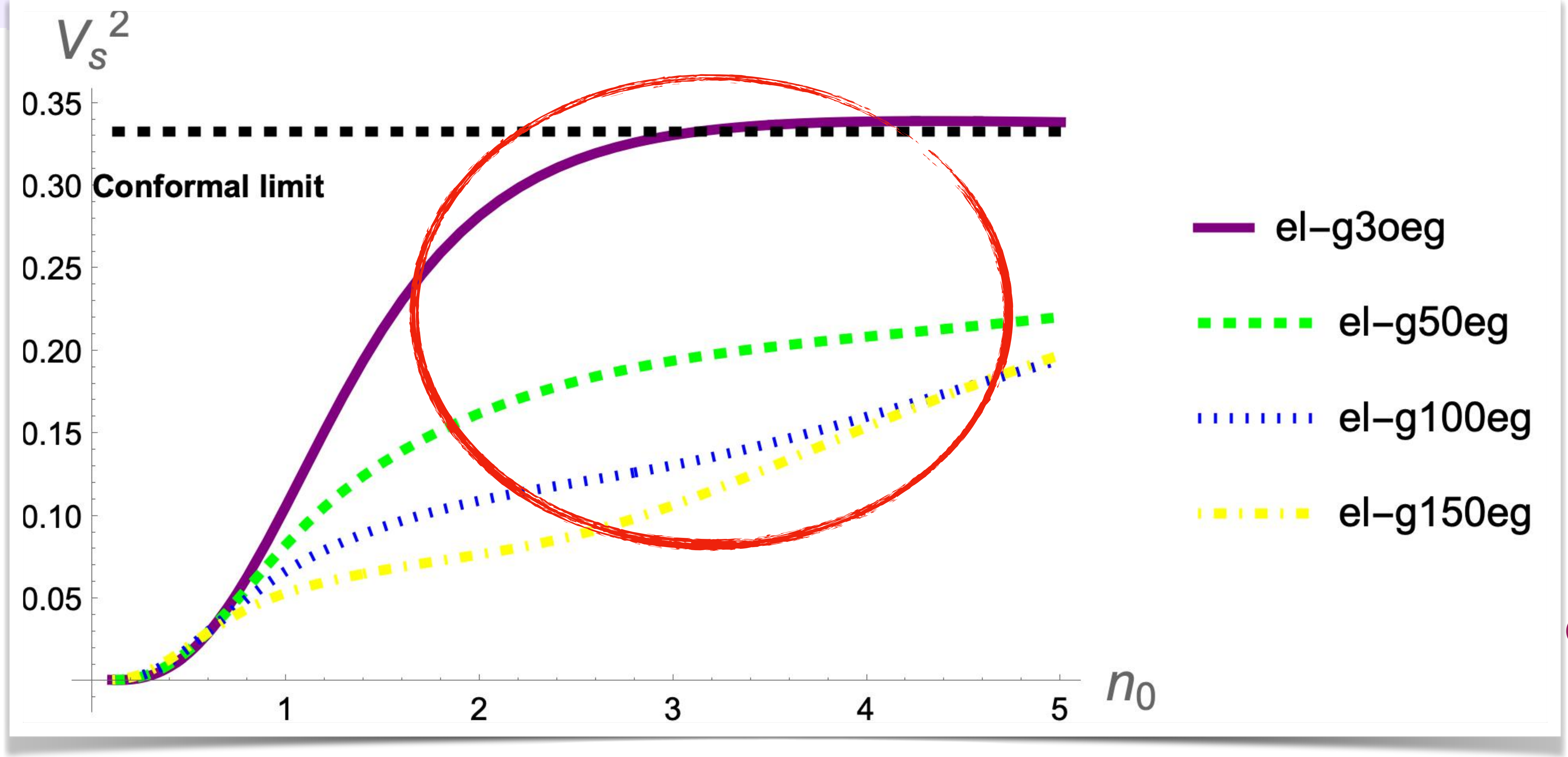

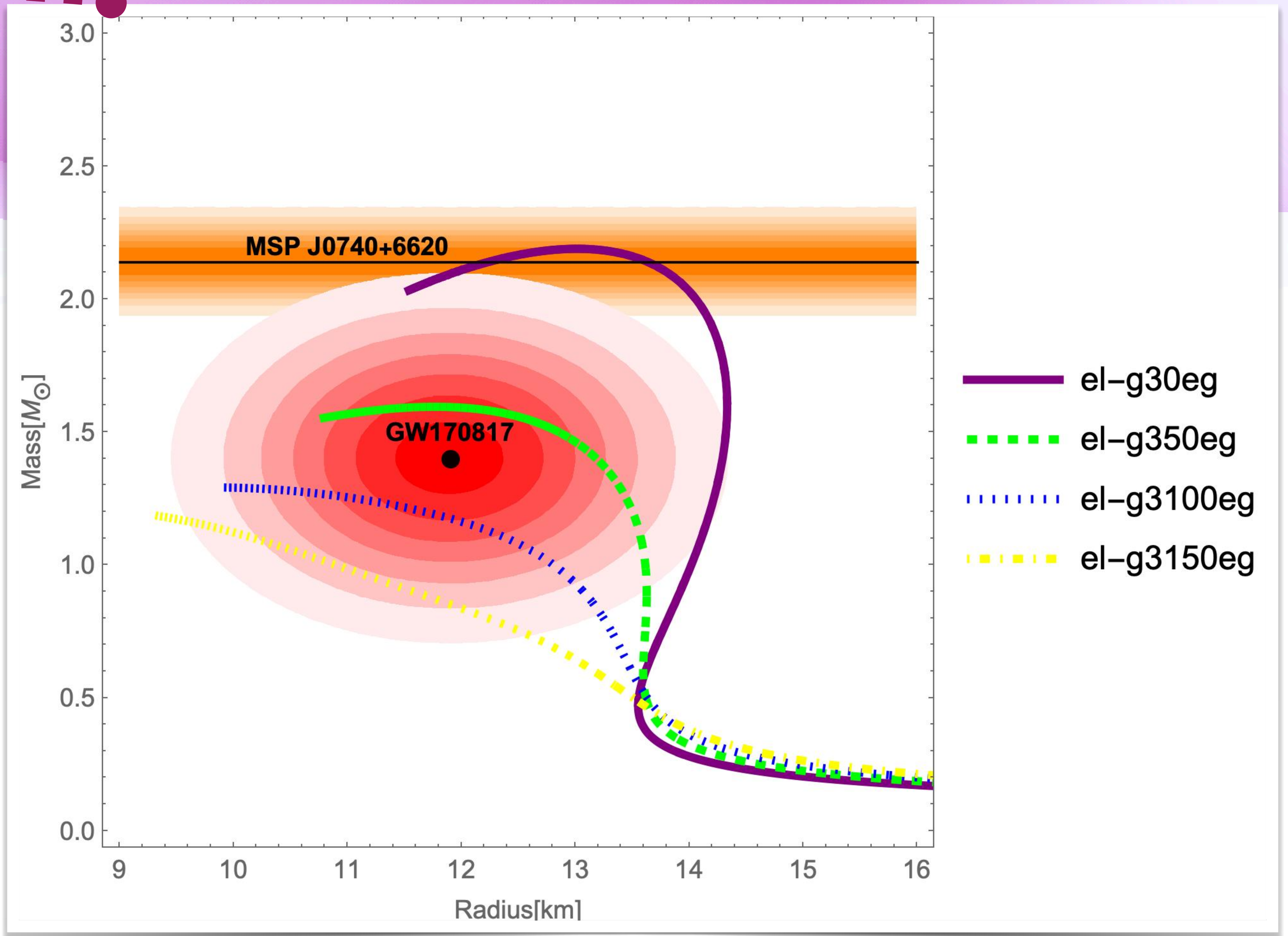

Comparison among different g_{aNN} cases

嚴謹求實
勤奮創新

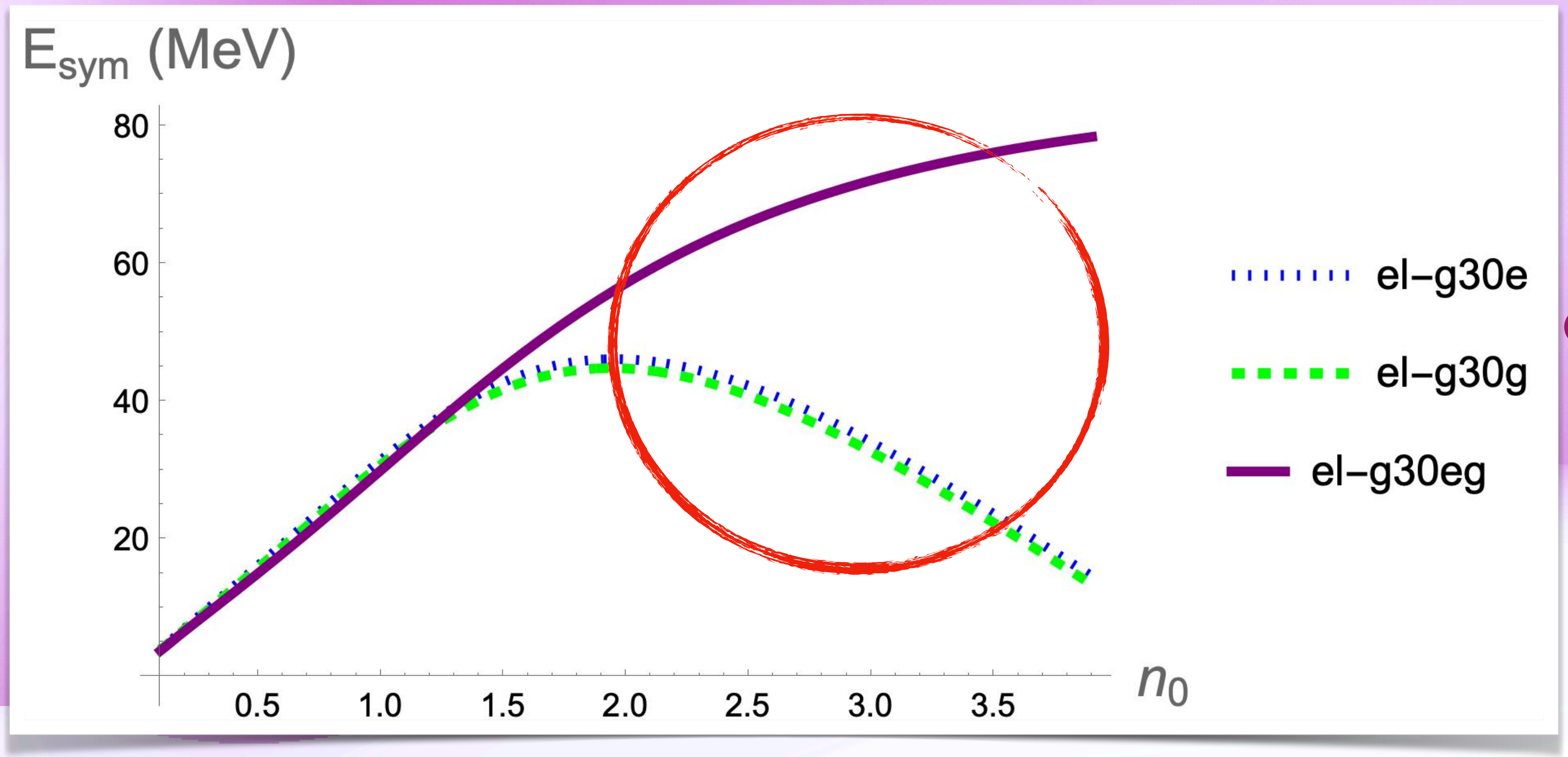

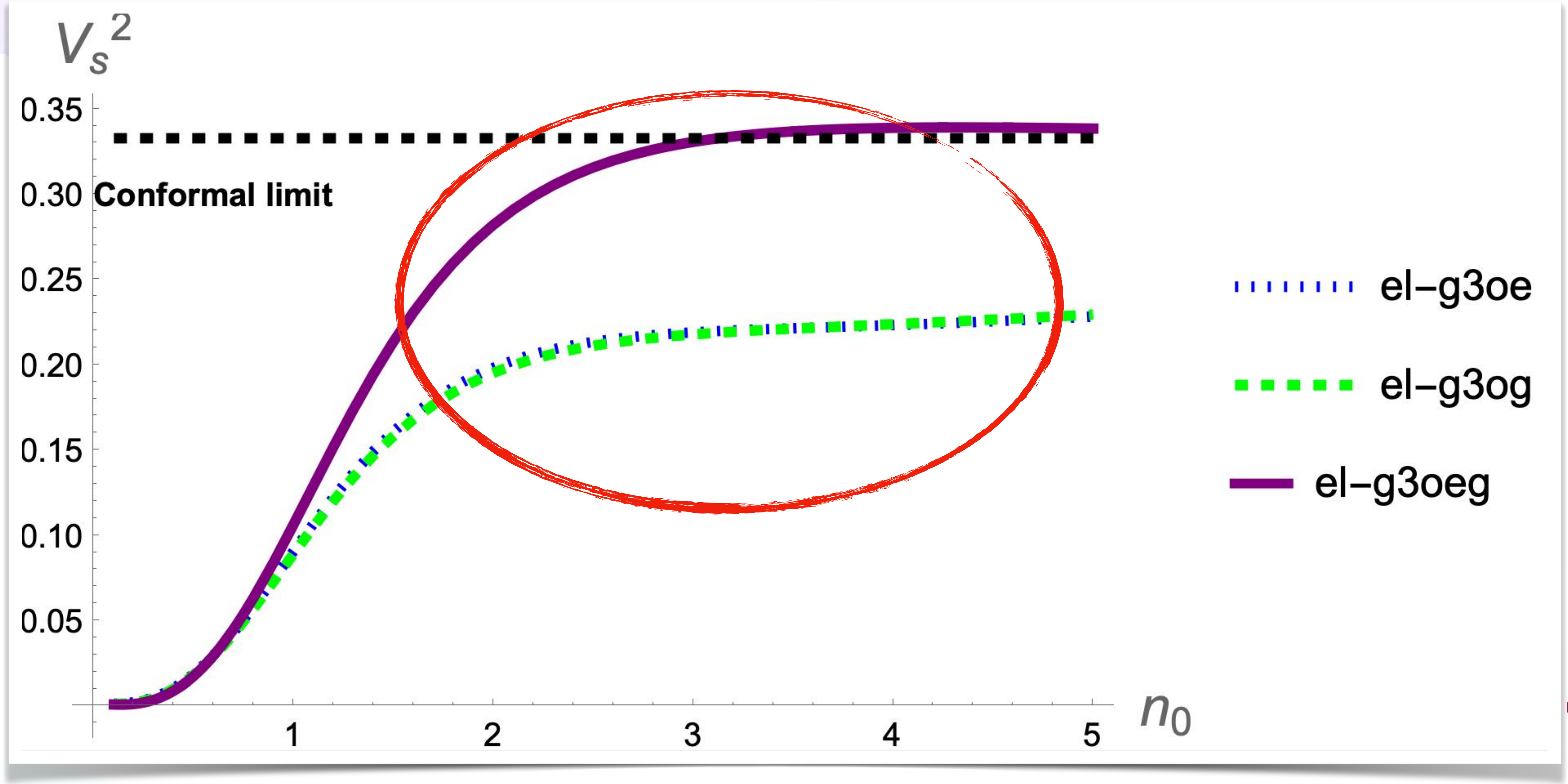

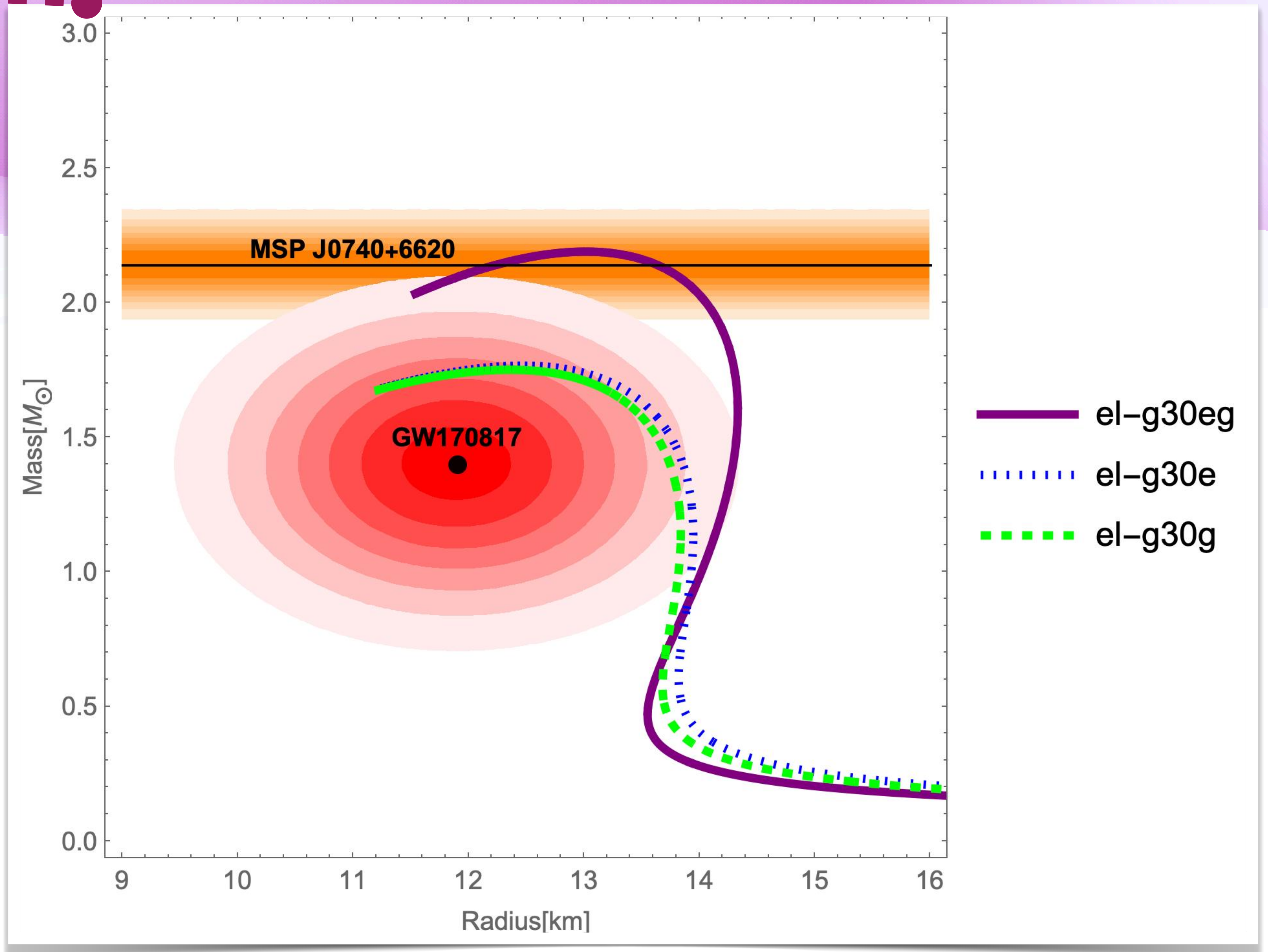

Comparison with Walecka-type models

Saturation density

A. Sedrakian, J. J. Li, and F. Weber, Prog. Part. Nucl. Phys. 131, 104041 (2023)

	Empirical	ELSM	TM1	$\mathrm{FSU}-\delta 6.7$
$n_0(\mathrm{fm}^{-3})$	0.155±0.005	0.155	0.145	0.148

Symmetric nuclear matter

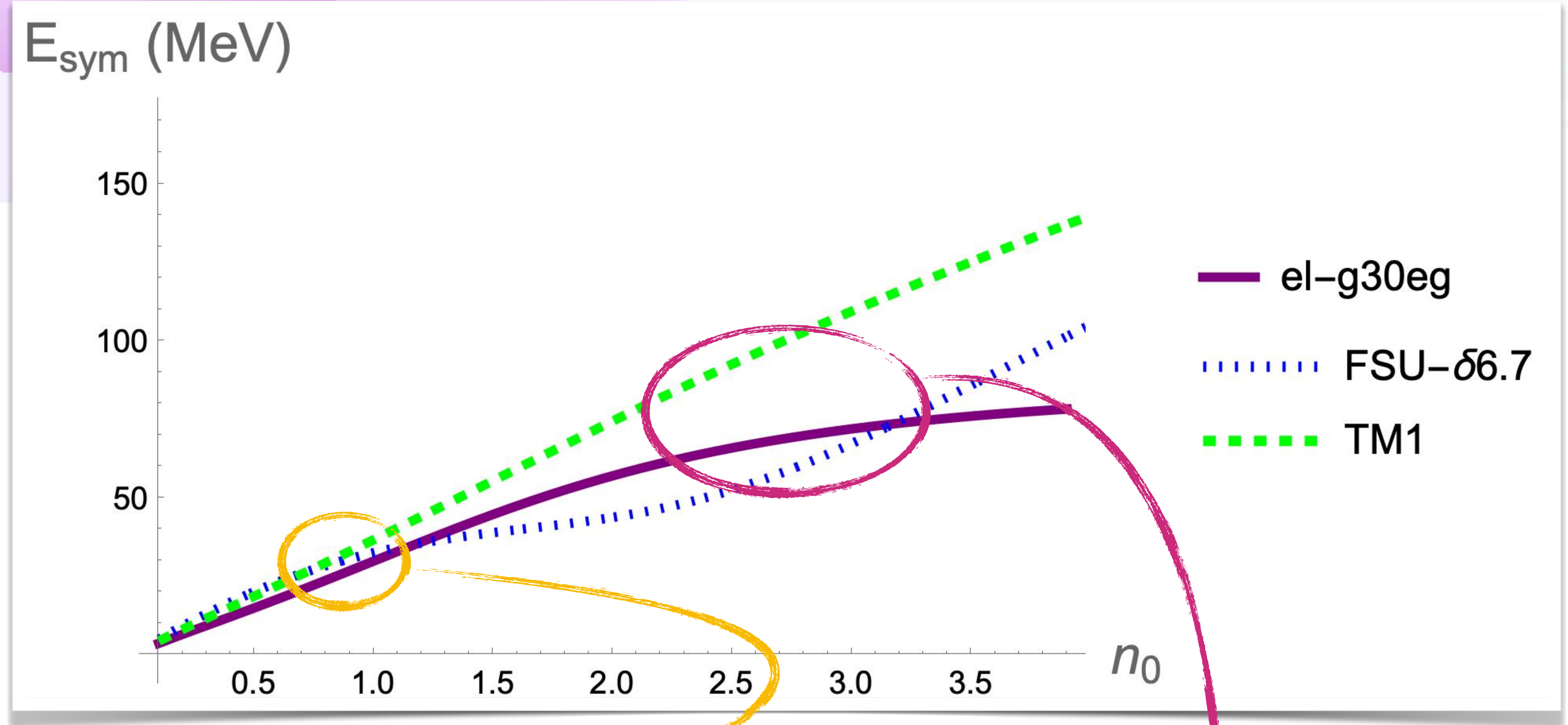

$L\left(2/3n_0\right) \geq 49\mathrm{MeV}$

GW170817 $\Lambda_{1.4} \leq 580$

Pure neutron matter

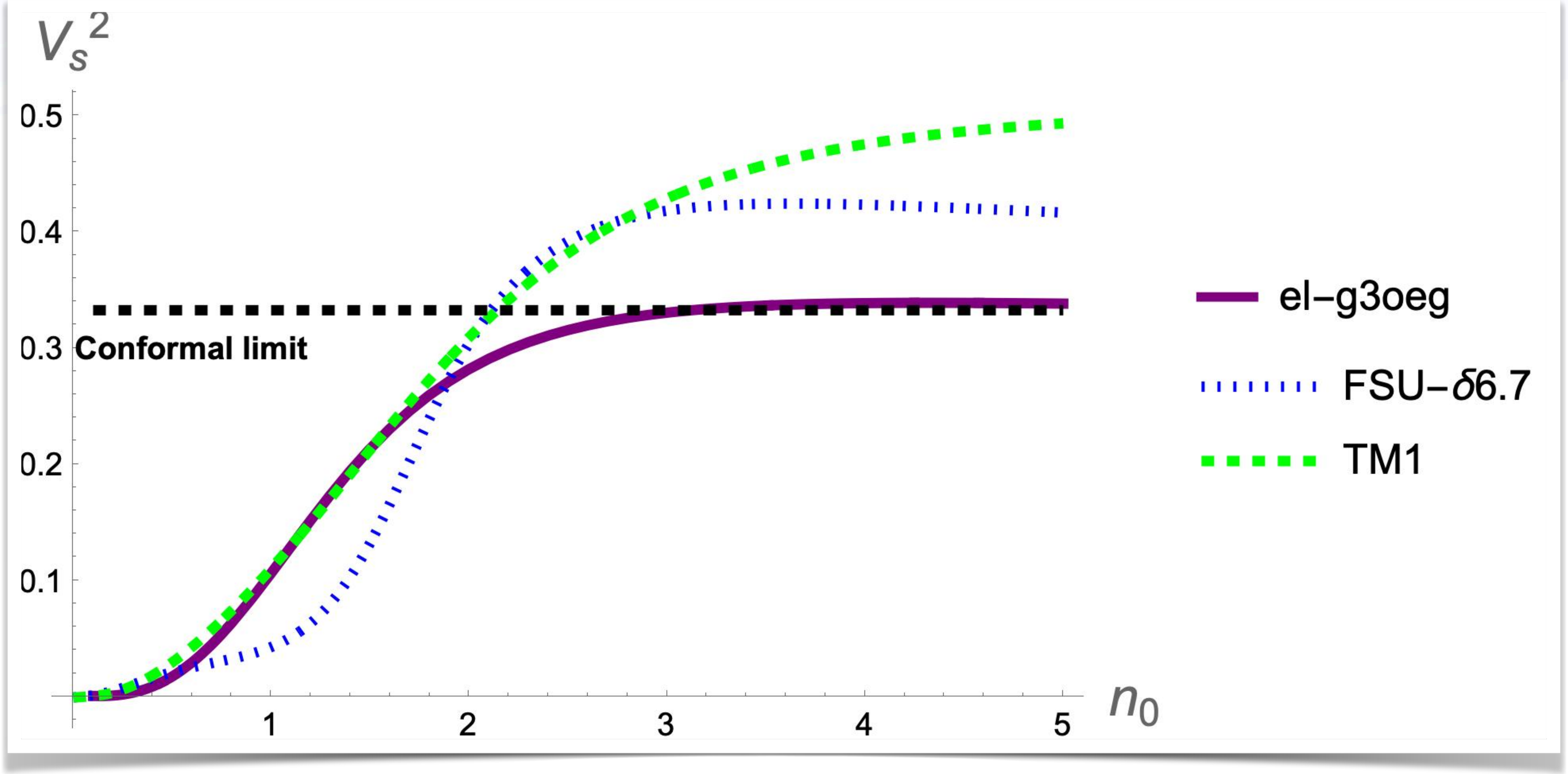

D. Adhikari et al., PREX, Phys. Rev. Lett. 126, 172502 (2021)
B. T. Reed, F. J. Fattoyev, C. J. Horowitz, and J. Piekarewicz, Phys. Rev. Lett. 126, 172503 (2021)
B. P. Abbott et al., LIGO Scientific, Virgo, Phys. Rev. Lett. 121, 161101 (2018)

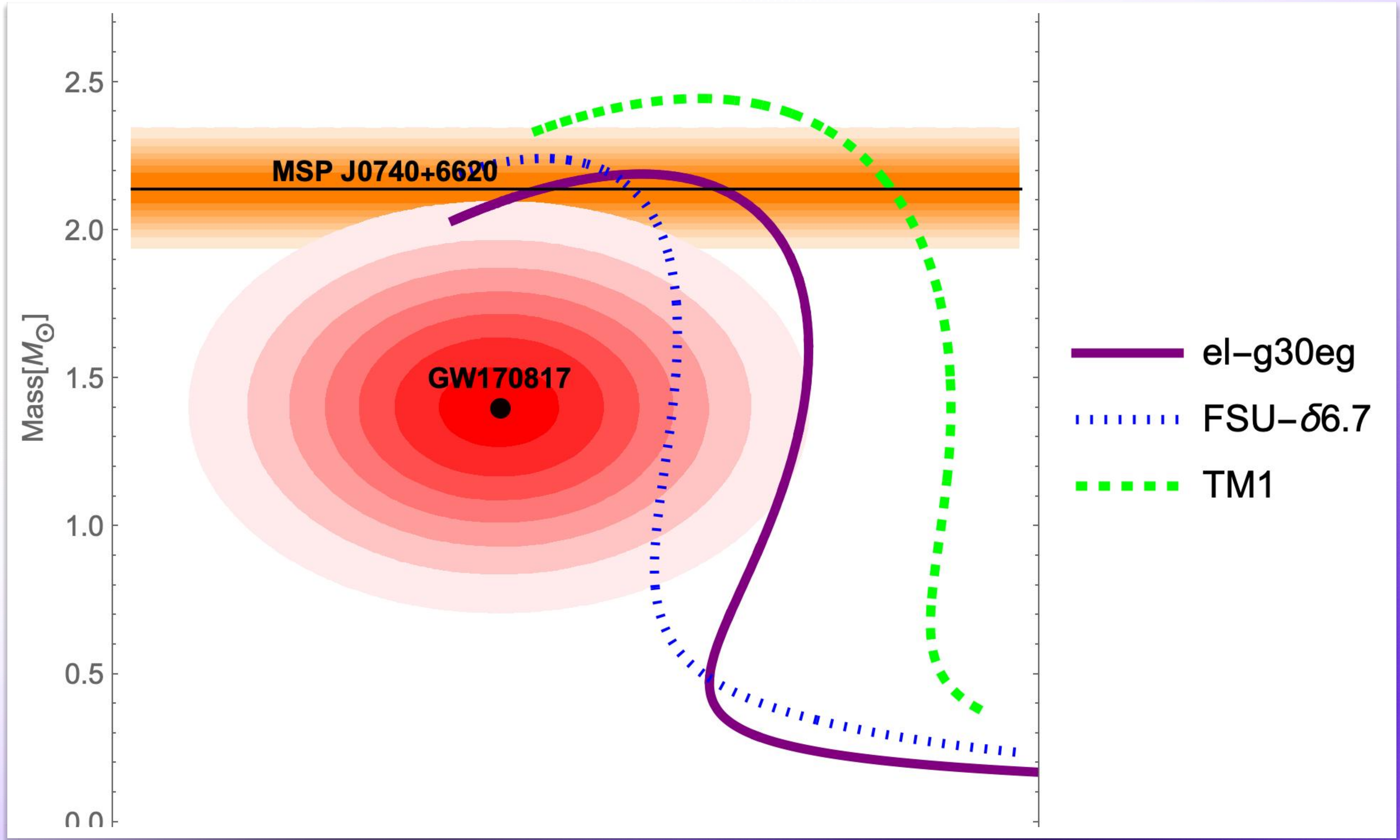
2.5
2.0
1.5
1.0
0.5
0.0
Mass[$M_\odot$]
MSP J0740+6620
GW170817
el−g30eg
FSU−δ6.7
TM1

The percentage of 2/4-quark configuration of scalar mesons

	σ		δ	
	p_4	p_2	p_4	p_2
el-g30g	51.7%	48.3%	77.9%	22.1%
el-g30e	51.2%	48.7%	77.2%	22.8%
el-g30eg	54.2%	45.8%	81.5%	18.5%
el-g350eg	52.4%	47.6%	77.3%	20.7%
el-g3100eg	49.2%	50.8%	74.4%	25.6%
el-g3150eg	48.9%	51.1%	74.3%	25.7%

Slight difference of configurations
but large difference at macroscopic level

The scalar meson couplings from different approaches

MeV

	$C_{\sigma\delta^2}$	$C_{\sigma^2\delta^2}$
Zabari-19	± 1.77	± 0.004
FSU-δ6.7	—	2.63
el-g30g	-1860	-9.40
el-g30e	-1940	-9.71
el-g30eg	-1480	-7.70
el-g350eg	-1690	-8.75
el-g3100eg	-2190	-11.0
el-g3150eg	-2160	-11.0

N. Zabari, S. Kubis, and W. Wójcik, Phys. Rev. C 99, 035209 (2019)
F. Li, B.-J. Cai, Y. Zhou, W.-Z. Jiang, and L.-W. Chen, Astrophys. J. 929, 183 (2022).

Quite different parameter space!

Summary and outlook

I. The EFTs/models of low energy QCD can reproduce the NM properties and NS structures;

II. Regarding the well-reproduced vacuum spectra and NM properties at low densities, different parameter space choices significantly affect the neutron star (NS) structure;

III. These astrophysical objects may serve as a promising test field for strong interaction theories/models, with more detailed analysis forthcoming (the connections between microscopic symmetry and macroscopic observations).

Strangeness in this framework

In collaboration with Lu-Qi Zhang (张璐琦)

南京大學

Explicit chiral symmetry breaking due to quark mass

$$\mathscr{L}_{\text{S.B.}} = -b_1 \operatorname{Tr}\left(\xi S^3\right) - G \operatorname{Tr}\left(\xi S\right) + b_2 \operatorname{Tr}\left(V^2 \xi S\right) + b_3 \epsilon^{ijk}\epsilon^{lmn}(V)_{il}(V)_{jm}\left(\xi S\right)_{kn}$$

$$-b_4 \operatorname{Tr}[\bar{B}\xi B] - b_5 \epsilon^{ijk}\epsilon^{lmn}(\bar{B})_{il}(\xi)_{jm}(B)_{kn}$$

$$\xi = \xi_1\lambda_1 + \xi_3\lambda_3 + \xi_8\lambda_8$$

Non-zero $\langle a_0 \rangle$ and $\langle f_0 \rangle$

Gell-Mann Okubo Formula

$$m_{\Sigma^+} = \frac{1}{2}\left(-2m_n + 3m_\Lambda - 2m_{\Xi^-} + 3m_{\Sigma^0}\right)$$

$$m_{\Sigma^-} = \frac{1}{2}\left(2m_n - 3m_\Lambda + 2m_{\Xi^-} + m_{\Sigma^0}\right)$$

$$m_{\Xi^0} = -m_n - m_p + 3m_\Lambda - m_{\Xi^-} + m_{\Sigma^0}.$$

$$m_{a_0}^2 + m_{f_0}^2 = 2m_\sigma^2$$

Analysis about NS is on the way

Thank you!